antibody binding (**Fig. 2(d)**). This finding supported the hypothesis that removing or trimming down the glycan shield of the spike antigen could elicit different immune responses against SARS-CoV-2 and greater efficacy against VOCs.

In summary, trimming the glycan shield of the spike protein to mono-GlcNAc glycoform enabled the conserved epitopes to be exposed to the immune system, leading to improved elicitation of more effective and broadly protective immune response against SARS-CoV-2 VOCs. Moreover, taking the broadly neutralizing m31A7 antibody in this study as an example, these targeted conserved epitopes could facilitate next-generation vaccine antigen design and development. (Reported by Han-Yi Huang, École Polytechnique Fédérale de Lausanne, Switzerland)

*This report features the work of research groups led by Chi-Huey Wong, Che Ma and Kuo-I Lin published in Sci. Transl. Med.* ***14****, eabm0899 (2022).*

### TLS 15A1 Biopharmaceuticals Protein Crystallography

- X-ray Crystallography, Biological Macromolecules
- Protein Structures, Nucleotides, Viral Defense, Life Science

### Reference

1. H.-Y. Huang, H.-Y. Liao, X. Chen, S.-W. Wang, C.-W. Cheng, M. Shahed-Al-Mahmud, Y.-M. Liu, A. Mohapatra, T.-H. Chen, J. M. Lo, Y.-M. Wu, H.-H. Ma, Y.-H. Chang, H.-Y. Tsai, Y.-C. Chou, Y.-P. Hsueh, C.-Y. Tsai, P.-Y. Huang, S.-Y. Chang, T.-L. Chao, H.-C. Kao, Y.-M. Tsai, Y.-H. Chen, C.-Y. Wu, J.-T. Jan, T.-J. R. Cheng, K.-I. Lin, C. Ma, C.-H. Wong, Sci. Transl. Med. **14**, eabm0899 (2022).

# How Binding of CDN to STING Reduces Phage Propagation in Bacteria

*This crystallographic analysis of the complex structures of PcSTING and MySTING with cyclic di-GMP elucidated how cyclic dinucleotide (CDN) was recognized and revealed the driving force behind filament formation.*

Mammalian STimulator of INterferon Genes (STING) is essential to innate immunity. During viral infection, the enzyme cyclic GMP–AMP synthase (cGAS) acts as a sensor that rapidly recognizes foreign nucleic acid molecules and synthesizes 2′3′-cGAMP as a second messenger. The binding of 2′3′-cGAMP to the STING dimer triggers its further oligomerization into filamentous structures, which in turn activate downstream effectors. Similarly, to combat viruses, the cyclic-oligonucleotide-based antiphage signaling system[1] in the bacterial arsenal consists of a cGAS/DncV-like nucleotidyltransferase (CD-NTase) that synthesizes diverse cyclic dinucleotide (CDN) and cyclic trinucleotide second messengers upon phage infection and an effector protein that binds to the CD-NTase product and induces programmed cell death through its various activities. The signaled suicide commitment serves as a defense strategy that restricts phage propagation. Recently, STING protein was revealed to be enlisted by bacteria.[2] In fact, eukaryotic STING has an origin in bacteria. Although mammalian STING has been investigated in detail, the three-dimensional structure of bacterial STING, the precise mode through which CDN binds to the dimeric protein, and the specific recognition mechanism have not yet been elucidated. In this work, a research team led by Yeh Chen (China Medical University) determined the C-terminal domain structures of *Pc*STING from *Prevotella corporis* and *My*STING from *Myroides sp.* ZB35 by using multiwavelength anomalous dispersion and molecular replacement methods with data collected from SeMet-labeled and CDN-bound crystals at beamlines **TPS 05A**, **TPS 07A**, and **TLS 15A1** of the NSRRC.[3]

The crystals of *Pc*STING and *My*STING belong to the space groups $P2_12_12$ and $P2_1$, respectively; in both these groups, an asymmetric unit contains one dimer. The structures were refined to 2.25 and 2.17-Å resolution, and the coordinates were deposited in the PDB under accession codes 7EBD and 7EBL. The protomers in the *Pc*STING and *My*STING crystals had root-mean-square deviations (RMSDs) of 0.29 and 0.64 Å for 158 and 160 matched Cα pairs, respectively, with the STING domain forming canonical V-shaped dimers (**Figs. 1(a) and 1(b)**, see next page). Each protomer has a mixed α/β fold with a central five-stranded β-sheet surrounded by five α-helices and a flanking β-ribbon.

The *Pc*STING and *My*STING dimers are similar and have an RMSD of 1.09 Å for 272 Cα pairs. The electron density maps unambiguously identified the bound CDN as cyclic-di-GMP (CDG; **Figs. 1(c) and 1(d)**), which originates from the expression host and is copurified with the protein, as verified through mass spectroscopic analysis. Recognition of the CDG, bound in a symmetric manner to the dimeric protein, is dictated by interactions of the guanine base with the side chains of Arg233/Asp252 and the backbone of His238 in *Pc*STING (conversely, Arg230/Asp251 and His235 in *My*STING; **Fig. 1(e)**). In addition, each nucleobase of the CDG is sandwiched by Phe171 of one *Pc*STING protomer and Tyr235 of the other *Pc*STING protomer, and there are extensive π–π stacking interactions (Leu169 and Tyr232 in *My*STING; **Fig. 1(f)**). The aromatic tyrosine side chain also interacts with the planar guanidinium group of Arg233, creating a unique Phe/Gua/Tyr/Arg four-layer double-stack formation supported by the hydrogen bonds between Arg233/Asp252 and the CDG (**Fig. 1(g)**). The binding mode was challenged by mutating Tyr232 into Arg in *My*STING. The affinity of binding to CDG was measured using isothermal titration calorimetry and was revealed to be nearly 1200 times lower than in the wild type.

The binding of CDG to the STING domain of full-length TIR-STING can induce TIR oligomerization into long filament and activate the $NAD^+$ cleavage activity of its TIR domain. The subsequent depletion of $NAD^+$ results in cell death. In fact, overexpression of wild-type *Pc*TIR-STING or *My*TIR-STING in *Escherichia coli* was discovered to result in considerable growth inhibition, and mutating the specificity determining residue Arg233 or Asp252 in *Pc*TIR-STING reversed this growth inhibition, thereby validating the amino acid's vital roles in CDG recognition. Moreover, the oligomerization state is implicated in the crystal structures of both *Pc*STING and *My*STING. Each V-shaped dimer of *Pc*STING associates with its neighbors on both sides, which are symmetry-related through unit-cell translation along the *c*-axis (**Figs. 2(a) and 2(b)**). A similar arrangement of dimers along the *a*-axis of the *My*STING crystal suggests a common mode of dimer–dimer interaction (**Figs. 2(c) and 2(d)**). The interface excludes surface area of size 1440 $Å^2$ on the *Pc*STING dimer (1420 $Å^2$ on *My*STING), which is comparable to the subunit interface of 1120 $Å^2$ (1500 $Å^2$) in a dimer. If a continuous filament subsequently forms, each dimer has nearly 10% of its surface area buried, and at least 60 amino acid residues are involved (**Fig. 2(e)**). The oligomerization is stabilized by the highly complementary molecular shapes and electrostatic charges at the interface. In addition to large hydrophobic patches, specific interactions such as the salt bridges of Lys212-Asp301 and Lys220-Glu306 and the hydrogen bond of Ser213-Ser302 were observed in the *Pc*STING oligomer, and similar bonds were also present in *My*STING. However, mutations in these regions of *My*TIR-STING resulted in the aggregation of improperly formed oligomers.

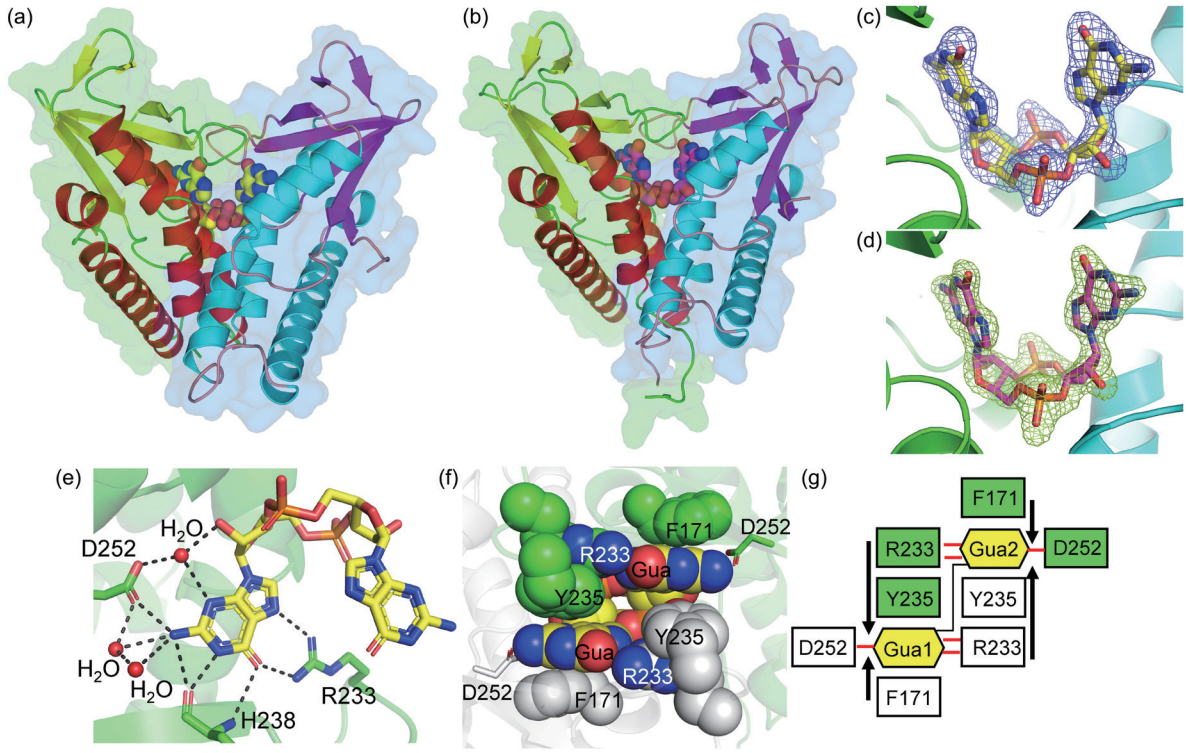


**Fig. 1**: Structures of bacterial STING in a complex containing cyclic di-GMP. Surface and cartoon models of (a) *Pc*STING and (b) *My*STING dimers are presented, with colors differentiating the two protomers. The cyclic di-GMP is depicted as a space-filled model. The $F_o$–$F_c$ maps for the ligand binding to (c) *Pc*STING and (d) *My*STING are contoured at the 4-σ level. The hydrogen bonding network and stacking interactions between *Pc*STING and cyclic di-GMP are depicted in (e) and (f) and further illustrated in a diagram (g). [Reproduced from Ref. 3]

In summary, this study elucidated the precise binding mode of bacterial STING and the cognate ligand CDG by performing X-ray crystallography. The symmetrical interactions determine the specificity for CDG, which differs from the specificity for CDN of other STING complexes such as 2′3′-cGAMP. The crystal structures further provide a plausible mode of STING oligomerization, which is vital to STING's biological function. (Reported by Tzu-Ping Ko, Academia Sinica)

*This report features the work of Yeh Chen and his colleagues published in Nat. Commun.* ***13****, 26 (2022).*

**TPS 05A Protein Microcrystallography**
**TPS 07A Micro-focus Protein Crystallography**
**TLS 15A1 Biopharmaceuticals Protein Crystallography**

- X-ray Crystallography, Biological Macromolecules
- Protein Structures, Nucleotides, Viral Defense, Life Science

## References


1. A. Millman, S. Melamed, G. Amitai, R. Sorek, Nat. Microbiol. **5**, 1608 (2020).
2. B. R. Morehouse, A. A. Govande, A. Millman, A. F. A. Keszei, B. Lowey, G. Ofir, S. Shao, R. Sorek, P. J. Kranzusch, Nature **586**, 429 (2020).
3. T.-P. Ko, Y.-C. Wang, C.-S. Yang, M.-H. Hou, C.-J. Chen, Y.-F. Chiu, Y. Chen, Nat. Commun. **13**, 26 (2022).


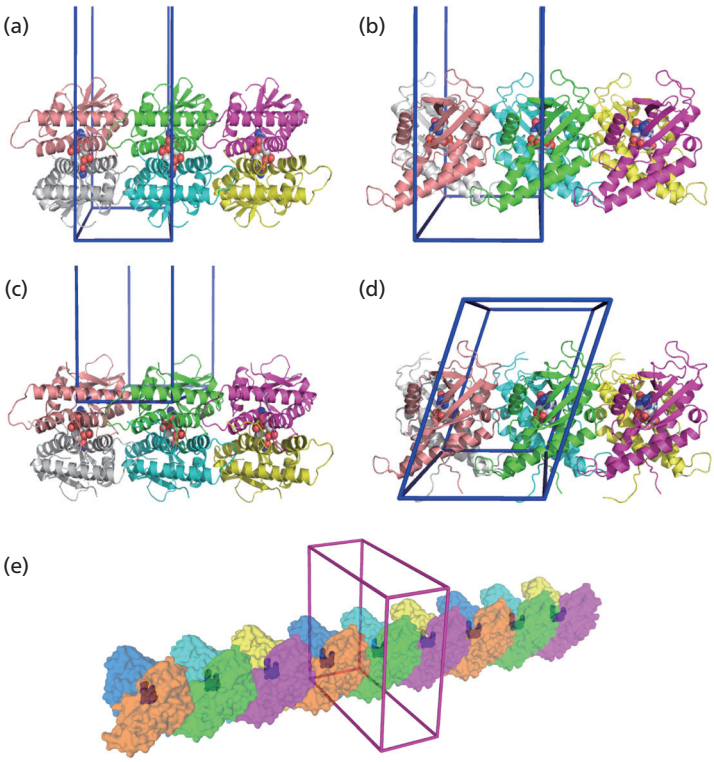


**Fig. 2**: Mode of bacterial STING oligomerization. Two orthogonal views of three juxtaposed dimers of *Pc*STING (a,b) and *My*STING (c,d) as viewed in crystals with color-differentiated protomers. The unit cells are depicted as cages. A diagram for the extended packing of the *Pc*STING crystal is depicted in (e) with color-differentiated translucent protein dimers. The bound CDG molecules are indicated in blue. [Reproduced from Ref. 3]

# Structural Analysis and Engineering of Aldo-Keto Reductase from Glyphosate-Resistant *Echinochloa colona*

***Glyphosate is the most widely used non-selective herbicide because of its high efficacy and low cost. Our study revealed the mechanism of aldo-keto reductase mediated glyphosate degradation and engineered a variant, which exhibited a 70% in glyphosate degradation.***

Since it was first registered for use as a pesticide in 1974, glyphosate has become the most commonly used organophosphate herbicide. It acts as a 5-enolpyruvylshikimate-3-phosphate synthase inhibitor to block the shikimate pathway and aromatic amino acid biosynthesis.[1] In most plants, glyphosate can be degraded to weakly phytotoxic aminomethyl phosphonic acid and glyoxylate;[2] the underlying mechanisms of this process remain poorly understood. In 2020, a glyphosate-resistant *Echinochloa colona* (*E. colona*) population from western Australia has been reported.[3] The elevated glyphosate degradation in *E. colona* is caused by the upregulation of two homologous aldo–keto reductases (AKRs), namely AKR4C16 and AKR4C17.[3] AKR4C16 and AKR4C17 are the first naturally-occurring glyphosate-degrading machinery reported in plants.

To explore the mechanism of AKR-mediated glyphosate-degradation, a research team led by Rey-Ting Guo (Hubei University, China) solved the apo-form and cofactor/glyphosate-bound structures of AKR4C17 from the glyphosate-resistant *E. colona*.[4] The X-ray diffraction data were collected at **TLS 15A1** and **TPS 05A** of the NSRRC. AKR4C17 displays a triose-phosphate isomerase barrel